ELSEVIER

Bone 42 (2008) 229–234

BONE

www.elsevier.com/locate/bone

Technical Note

Secondary ionization mass spectrometry imaging of dilute stable strontium labeling in dentin and enamel

Vincent Balter [a,*], Bruno Reynard [b]

[a] UMR 5125 "PaléoEnvironnements et PaléobioSphère", CNRS, France; Université Lyon 1, Campus de la DOUA, Bâtiment Géode, 69622 Villeurbanne Cedex, France

[b] UMR 5570 "Laboratoire de Sciences de la Terre", CNRS, France; Ecole Normale Supérieure de Lyon, Université Lyon 1, France

Received 9 May 2007; revised 27 July 2007; accepted 23 August 2007
Available online 6 September 2007

Abstract

The labeling of the zones of active mineralization in bone and tooth is usually achieved with calcium-binding fluorescent dyes. However, these compounds are labile and mostly lost during the maturation process of the growing tissue. Here we labeled mouse teeth using injections of dilute strontium ($SrCl_2$, 500 μg/ml), a trace element that is naturally incorporated in hydroxyapatite, and resolve the subtle induced compositional changes using secondary ion mass spectrometry (SIMS) imaging and analysis. Entire hemi-mandibules sampled at 14 and 28 days after birth are embedded in resin and polished along longitudinal sections. SIMS chemical imaging reveals the double Sr labeling both in dentin and enamel of molar teeth as two stripes with excess Sr concentration parallel to the dentino-enamel junction. In order to quantify the variations of the strontium/calcium ratio (Sr/Ca), two international standards were sintered and measured along with the samples. The concentration of Sr in the two stripes is about 300 μg/g, which corresponds to an enrichment factor of about 1.3–1.4 relative to the natural baseline. These results show that SIMS provides rapid and quantitative imaging of small abundances of stable isotopes in growing mineralized tissues with a sensibility that is at least two orders of magnitude higher than classical X-rays microanalysis.

Keywords: Stable isotope; Strontium; Secondary ionization mass spectrometry

Introduction

The labeling of the mineral phase (hydroxylapatite, HAP) of growing bone and teeth can be achieved with several techniques, each having specific side effects. Autoradiographic methods are used to localize and estimate the uptake of radionuclides in various growing tissues [1,2]. However, in addition to the fact that radioactive β emissions could locally destroy active cells, autoradiogram resolution depends on the energy of emitted β particles as well as sample thickness [3]. Semi-quantitative measurements of element concentrations can be achieved by means of X-ray microanalysis, but this technique remains restricted to the determination of major elements with typical concentrations around a few percents [4]. Fluorescent organic markers, such as the antibiotic family of tetracycline-derived compounds, are commonly used in experimental studies [5–7]. However, these large molecules are not incorporated into the HAP crystals, but are bound to their surfaces through a chelating process with calcium [8]. Fluorescent organic markers are thus labile compounds that are mostly lost during the maturation of the mineralized tissue.

Imaging of nonradioactive tracers by secondary ion mass spectrometry (SIMS) is an alternative technique, which was developed three decades ago for biological materials [9–15]. SIMS allows to image stable isotopes abundances with a theoretical detection limit of few ng/g and a spatial resolution of 0.5 μm. In spite of its analytical potential, the development of quantitative SIMS imaging in biomedical research has been hampered by the specific preparations of the samples, which involves specialized cryogenic techniques [11,12] or complex embedding procedures [14,15]. The aim of the present study is to demonstrate that quantitative imaging can be achieved by SIMS analysis with a very simple preparation of the samples. We show that SIMS allows to reconstruct the distribution of a double labeling of stable strontium in dentin and enamel with a

* Corresponding author.
E-mail address: Vincent.Balter@univ-lyon1.fr (V. Balter).

8756-3282/$ - see front matter © 2007 Elsevier Inc. All rights reserved.
doi:10.1016/j.bone.2007.08.037

spatial resolution of about 1 μm and a typical concentration of about 10^2 μg/g, which is at least two orders of magnitude lower than X-ray microanalysis.

Materials and methods

Experimental design

The protocol of animal experiments has been approved by the Ethic Committee of the PBES (Plateau Expérimental de Biologie de la Souris) at the Ecole Normale Supérieure de Lyon, France. Two pregnant mice are similarly labeled with three intraperitoneal injections of physiological serum doped with strontium (Sr) or barium (Ba). The two injections of Sr occur after 10 days and 17 days of gestation and the injection of Ba occurs after 14 days of gestation, respectively. This protocol has been adapted from the mouse dental mineralization schedule, which states that molars begin to mineralize during the second week *in utero* [16]. The injections are performed ahead of the dental mineralization schedule by few days in order to take into account for the reservoir effect created by the body mass of the gestating mouse and the offspring. The doped solutions are prepared from Sr and Ba chlorides to obtain final concentrations of 500 μg/ml. After birth, the animals are raised in normal conditions with food and water *ad libitum*. Half of the litter is sacrificed at 14 days and the remaining at 28 days.

Specimen preparation

Jaws are dissected from the animals and adjoining flesh is carefully removed. The specimens are stored in alcohol at room temperature. Clean hemi-mandibles are partially fixed in methanol, dehydrated and embedded in epoxy resin. They are sectioned longitudinally with a diamond wafering wheel saw. The resulting surfaces are gently polished manually on wet fine-grained sandpaper, and the specimens mounted on sample holders and gold-coated by vacuum deposition for SIMS analysis.

Apatite international standards preparation

Two international standards, one sedimentary HAP (francolite), NBS120c ("Florida Phosphorite" from the National Institute of Standards and Technology), and one biological HAP, SRM1400 ("Bone Ash" from the National Institute of Standards and Technology), are used for the internal standardization of the mass spectrometer. The chemical composition of the major constituents is given in the Table 1. About 100 mg of these powdered samples is sintered at high pressure (2 GPa) and high temperature (700 °C) in a belt apparatus at the Centre des Hautes Pressions of the Claude Bernard Lyon 1 University. The resulting solid samples are manually abraded and polished with wet fine-grained sandpaper in order to obtain clean and flat surfaces and, after mounting on sample holders, were gold-coated by vacuum deposition.

Table 1
Concentration of the certified and noncertified major constituents of the international standards NBS120c and SRM1400

	Concentration (wt.%)	
	NBS120c (Florida phosphate rock)	SRM1400 (Bone ash)
Si	2.57±0.093	(0.13)
Al	0.69±0.021	(530)[a]
Fe	0.76±0.021	660±27[a]
Mg	0.19±0.006	0.684±0.013
Ca	34.32±0.121	38.18±0.130
Na	0.39±0.015	(0.6)
K	0.12±0.003	186±8[a]
P	14.55±0.026	17.91±0.190
F	3.82±0.020	(0.12)
CO_3	4.46±0.164	–
Loss on ignition[b]	–	(0.87)
CaIP	2.36±0.009	2.13±0.024

Values in parenthesis are not certified.
[a] Unit in μg/g.
[b] 2 h at 1000 °C.

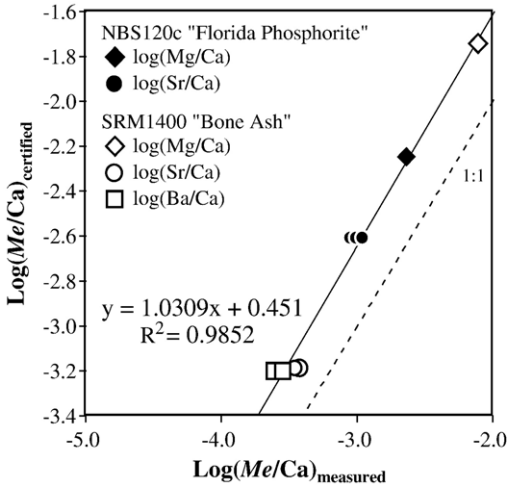

Fig. 1. Distribution of the certified metal/calcium ratio (*Me*/Ca) logarithm as a function of the measured ratio logarithm by SIMS in two apatite international standards, NBS 120c and SRM 1400. The equation of the linear regression is reported along with the 1/1 relationship.

SIMS analysis

A CAMECA IMS-4f ion microscope (ISTEEM, Montpellier II University), operating with an O^- primary ion beam, is used to monitor positive secondary ions. The samples are bombarded by an O^- primary ion beam accelerated through 15.2 kV. The sputtered ions are extracted into an electrostatic field and a magnetic sector, and the resulting ion currents studied at the mass peaks 25, 43, 88 and 138 for isotopes ^{25}Mg, ^{43}Ca, ^{88}Sr and ^{138}Ba, respectively. Data are normalized to ^{43}Ca in order to compensate for any instrumental derivation and/or irregularities on the sample surface. The two international standards are mounted on the sample holders and analyzed along with the teeth samples. By comparison to the measured and certified values of the international standards, this procedure allows the calculation of the absolute values of the ^{25}Mg/^{43}Ca, ^{88}Sr/^{43}Ca and ^{138}Ba/^{43}Ca ratios in teeth. The ^{25}Mg, ^{43}Ca, ^{88}Sr and ^{138}Ba stable isotope results of the apatites international standard (NBS120c and SRM1400) are presented in Fig. 1. The relationship between the measured and certified metal/calcium (*Me*/Ca) ratios is linear implying that no mass-dependent fractionation occurs during the measurement by the mass spectrometer. This relationship is highly significant (r^2=0.98) and can be used to calculate the absolute value of a measured *Me*/Ca ratio. Elemental ratios can be recalculated assuming average natural stable isotope ratios for all samples.

Results

^{138}Ba secondary ion mapping did not reveal any heterogeneity in dentin or in enamel consistent with our labeling protocol (data not shown). The absence of any ^{138}Ba signal suggests that the injected Ba is stored in the body of the gestating mice or cannot pass through the placenta.

An example of ^{43}Ca and ^{88}Sr secondary ion images is presented in Figs. 2B and C along with the corresponding optical micrograph (Fig. 2A). Both dentin and enamel were analyzed and displayed different response to the ion beam. The ^{43}Ca map (Fig. 2B) shows a fairly homogeneous dentin and a heterogeneous enamel. The

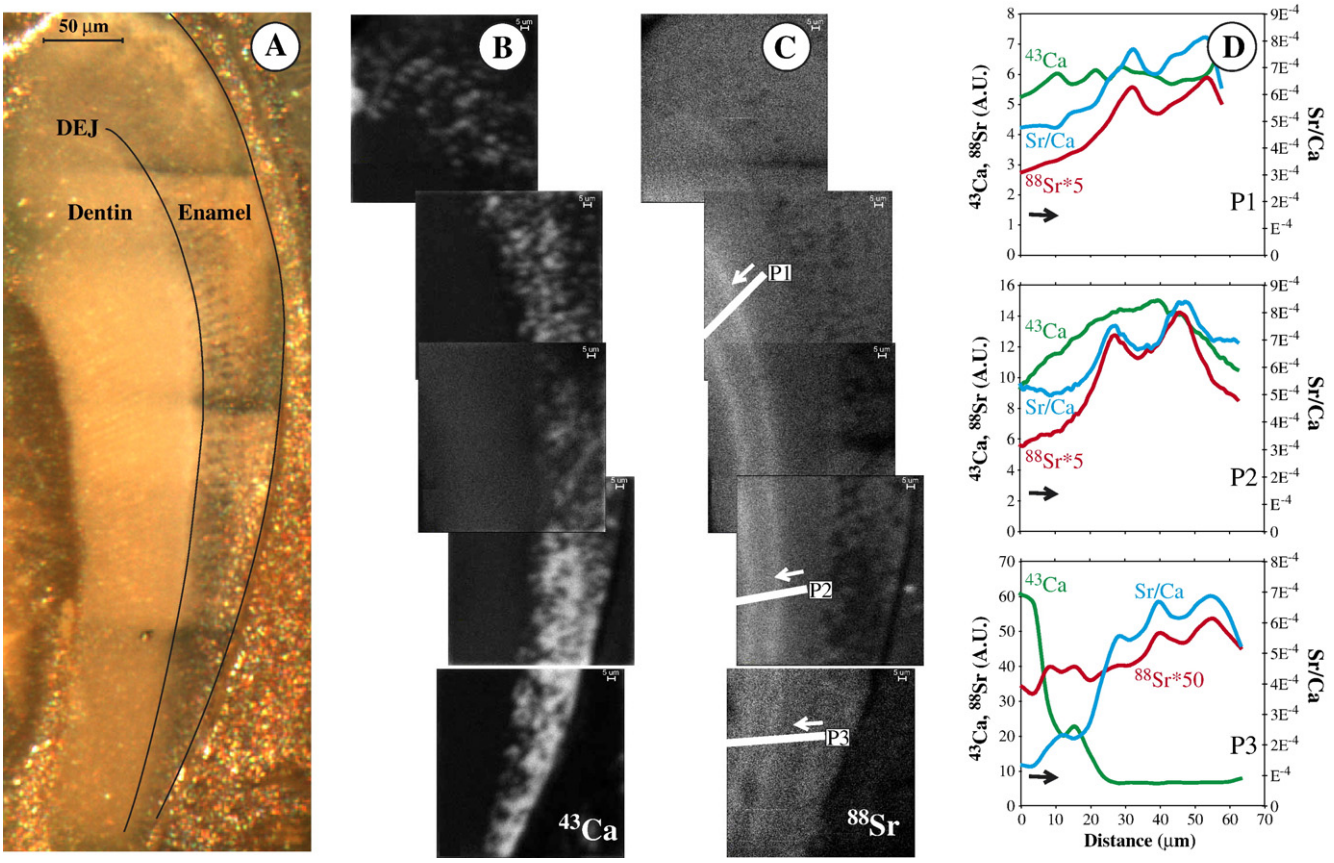

Fig. 2. (A) Optical micrograph of the posterior part of a 14 days old 2nd molar mouse which was analyzed by SIMS. Dentin, enamel and DEJ are reported. Decussating prisms are visible in enamel. (B) ^{43}Ca secondary ionic images. (C) ^{88}Sr secondary ionic images. The three line-scans are annotated P1, P2 and P3. The path of each line-scan is reported and the starting point indicated with a small arrow. (D) Sr/Ca ratios along the three line-scans shown in panel C. The Sr/Ca ratios are calculated using the natural isotopic abundances of ^{88}Sr (82.6%) and ^{43}Ca (0.13%) and normalized using the relationship defined in Fig. 1. ^{43}Ca and ^{88}Sr are reported in arbitrary units. The starting point of each profile is indicated with a small arrow.

homogeneous ^{43}Ca distribution in dentin suggests that the maturation process has been completed, because no gradient of mineralization, and thus of Ca concentration, can be observed as in the case when this tissue is maturing [17,18]. The homogeneity of dentin can also be explained by the limited intensity of the ^{43}Ca signal due to the low density of this tissue. The heterogeneity in enamel seems to occur at two levels, first in the enamel thickness and second in the crown height. The heterogeneity in enamel thickness is likely explained by either variable ion emission yield or charge effect on an irregular surface. Indeed, obtaining a flat surface is most challenging in enamel due to the existence of large crystalline fibers that can be ripped during polishing. The heterogeneity in crown height can be linked to the degree of mineralization of enamel in relation to the maturation cycles. The lower part of the crown exhibits a much more intense ^{43}Ca response in comparison to the upper part, a difference that can be explained by an active maturation banding in this area.

Sr labeling in the dentin at a tooth scale is readily imaged as two equidistant ^{88}Sr stripes that run subparallel to the dentino-enamel junction (DEJ). At the top of the molar where DEJ bends and where the dentin thickness is higher, the distance between DEJ and the stripes, and between stripes, increases in

Table 2
Sr/Ca ratios, Sr concentrations in the two labels and the respective baseline, and the corresponding Sr enrichment between each label and their baseline

		Baseline	1st label	1st label	Baseline	1st label	2nd label	1st label	2nd label
A14M1-P1	Dentin	0.48	0.76	0.80	191	306	319	60	67
A14M1-P2	Dentin	0.51	0.75	0.83	205	299	333	46	63
A14M1-P3	Dentin	0.23	0.67	0.68	90[a]	266	274	195[a]	204[a]
A14M2	Dentin	0.40	0.58	0.63	161	231	253	44	57
A14M3	Dentin	0.33	0.52	0.60	133	207	240	56	81
A21M1	Dentin	0.30	0.47	0.51	122	186	203	53	66
		0.38±0.11	0.62±0.12	0.68±0.12	162±36	249±49	270±49	52±7	67±9
A28M1	Enamel	0.17	0.32	0.44	68	129	177	89	160

[a] Badly defined baseline.

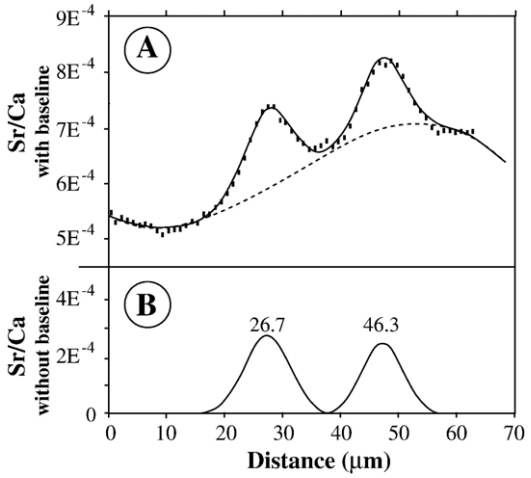

Fig. 3. (A) Sr/Ca line-scan of the profile P2 of the Fig. 2C. The overall Sr/Ca signal is deconvoluted into two peaks of Gaussian form centered at 26.7 µm and 46.3 µm, respectively (plain line), and a background fitted to a third-order polynome (dotted line). (B) Absolute Sr/Ca value of the two peaks after background substraction.

response to the corresponding increase of apparent apposition rate. The total Sr enrichment in the two labels and the apposition rates can be deduced from deconvolution of the ^{43}Ca and ^{88}Sr line-scans. If the profile P2 in Fig. 2D is considered, the two Sr/Ca peaks have a height of 2.4×10^{-4} and 3.2×10^{-4}, respectively (Table 2). Assuming that the Ca content in HAP is stoichiometric near 40 wt.%, this leads to a Sr enrichment of 46% and 63% in the two labels as compared to normal dentin. Considering a Sr/Ca baseline of 5×10^{-4}, a Sr concentration of 205 µg/g, 299 µg/g and 333 µg/g can thus be calculated for the baseline and the two labels, respectively. Five out of six of the analyzed specimens of dentin give similar results with a first Sr enrichment of 52±7% and a second Sr enrichment of 67±9% (Table 2). The increase of the Sr enrichment in the second label relative to the first is due to the fact that the latter peak is rooted in the former one. For the six analyzed specimens, the two Sr-enrichments lead to a Sr concentration of 249±49 µg/g and 270±49 µg/g in the first label and in the second label, respectively. This rather small variability suggests that our experiment gives reproducible results. It should be noted that variation of the Ca content does not change the Sr enrichment values. In contrast, an increase of 1% of the Ca content induces an increase of 5, 7 and 8 µg/g for the Sr

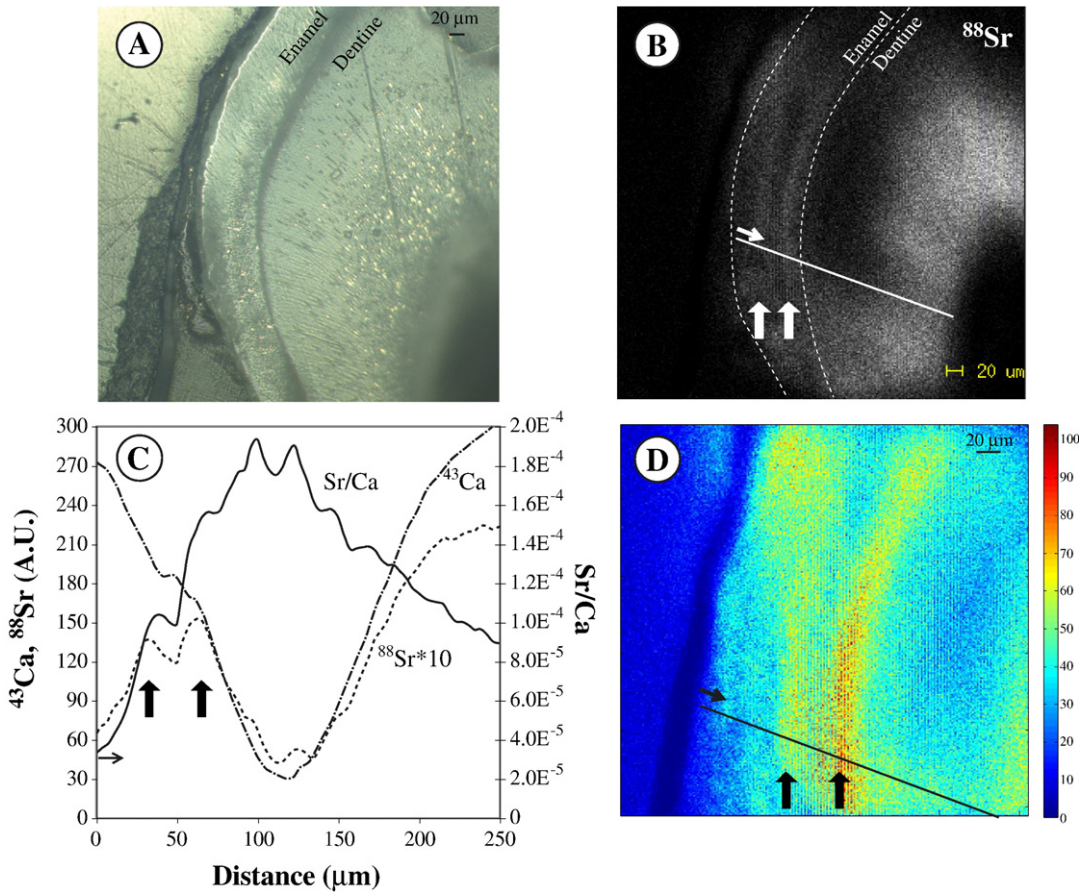

Fig. 4. (A) Optical micrograph of the anterior part of a 28 days old 1st molar mouse. Dentin and enamel are reported. (B) ^{88}Sr secondary ionic image reconstruction. Dentin, enamel and DEJ are reported and the two labels indicated by large arrows. The path of the line-scan is reported and the starting point indicated with a small arrow. (C) Sr/Ca ratios along the line-scan shown in panel B. The Sr/Ca ratios are normalized using the relationship defined in Fig. 1. ^{43}Ca and ^{88}Sr are reported in arbitrary units. The starting point of the profile is indicated with a small arrow. Note that the two Sr/Ca peaks that are identified at 100 and 125 µm, are characterized by very weak ^{88}Sr and ^{43}Ca signals associated with charge effects in the central area of the image. (D) Reconstructed first-derivative image of the Sr concentration calculated on each pixel of panel B.

concentration in the baseline, first label and second label, respectively.

A precise measure of the distance between the Sr bands of 19.6 μm can be obtained by deconvoluting of the overall signal (Fig. 3). Knowing that the interval between injection was 7 days, a dentin apposition rate of 2.8 μm/day is calculated, in accordance with published values reported in mammals for the dentin of tooth of limited growth [19]. The apposition rate varies slightly along the tooth, e.g. P1 and P3 profiles, by ca. 10% according to the variations of the apparent thickness of the dentin.

A secondary ion image showing our ^{88}Sr labeling in enamel is presented in the Fig. 4. The two ^{88}Sr stripes are parallel to the DEJ and located in the middle part of the analyzed area. In the line-scan, the corresponding two ^{88}Sr peaks are located at 40 and 70 μm. When the Sr/Ca signal is considered, the interpretation of the results is made difficult because of the strong variations in Ca within enamel and dentin. However, assuming a Ca content in HAP of about 40 wt.% leads to a Sr enrichment of about 61 μg/g and 109 μg/g in the two labels, respectively, as compared to normal enamel. The Sr concentration measured in enamel is about half that in dentin (Table 2), a pattern that is in accordance with *in natura* data [20].

Discussion

We emphasize that SIMS secondary imaging is a powerful tool for the localization of low concentrated stable isotope labeling in growing tissues. For example, it has been shown that Sr administration at low dose reduces bone resorption and increases bone formation, leading to an increase of the bone mass in normal and ovariectomized rats [21,22]. This has suggested a therapeutic potential for Sr in the treatment of osteoporosis, which was first tested in monkeys [23,24], using a range of oral Sr ranelate from high dose level (1 g/day/kg) to low dose level (0.1 g/day/kg). The resulting Sr distribution in bone was monitored by means of X-ray microanalysis, but accurate results seem to have been obtained only with monkeys fed with high dose of Sr ranelate. Oral Sr ranelate (2 g/day) has been shown to reduce vertebral and nonvertebral fracture risk in postmenopausal women with osteoporosis [25–27]. This dose level is about 30 mg/day when expressed by kg. Given that the intestinal absorption of Sr ranelate is different in monkeys and humans, direct and definitive comparison between these two species cannot be achieved, but this example shows that SIMS could be a fruitful technique for the study of the distribution of Sr at low concentration in bones.

Conclusions

This study shows that low concentrations of stable isotopes can be used to label the mineral phase of growing dentin and enamel. The tracer distribution is studied by SIMS secondary ionic imaging. The labeling technique is not associated with side effects related to the quality and/or quantity of the marking substance, as could be the case with fluorescent organic markers and radionuclides. We used a $SrCl_2$ solution with natural Sr isotope abundances, but the labeling tracer could be isotopically enriched to allow the labeling of growing tissues with low-abundance stable isotopes of elements (i.e. ^{25}Mg, ^{46}Ca, ^{58}Fe or ^{67}Zn). Such a technique would open up perspectives for the comprehension of the mineral metabolism of essential trace elements and the study of the distribution of depleted elements.

Acknowledgments

We would like to thank N. Aguilera for the mice growing and handling, and for the preparation of the jaw samples, and B. Boyer for the SIMS analysis. We also thank two anonymous reviewers and the Associate Editor David B. Burr for their helpful comments. This work is supported by the Institut National des Sciences de l'Univers through the ECLIPSE program and SIMS national instrument in Montpellier. This is contribution UMR5125-07.035.

References

[1] Vincent J. Distribution of sodium in compact bone, as revealed by autoradiography of neutron-activated sections. Nature 1959;184:1332–3.
[2] Moran RA, Deaton TG, Bawden JW. Problems associated with estimation of net calcium uptake during enamel formation using 45Ca. J Dent Res 1995;74:698–701.
[3] Glenn HJ. Biologic applications of radiotracers. Boca Raton: CRC Press; 1982.
[4] Boivin G, Deloffre P, Perrat B, Panczer G, Boudeulle M, Mauras Y, et al. Strontium distribution and interactions with bone mineral in monkey iliac bone after strontium salt (S 12911) administration. J Bone Miner Res 1996;11:1302–11.
[5] Milch RA, Rall DP, Tobie JE. Bone localization of the tetracyclines. J Nat Cancer Inst 1957;19:87–93.
[6] Owen IN. Fluorescence of tetracyclines in bone tumors, normal bone and teeth. Nature 1961;190:500–2.
[7] Pautke C, Vogt S, Tischer T, Wexel G, Deppe H, Milz S, et al. Polychrome labeling of bone with seven different fluorochromes: enhancing fluorochrome discrimination by spectral image analysis. Bone 2005;37:441–5.
[8] Kohn KW. Mediation of divalent metal ions in the binding of tetracycline to macromolecules. Nature 1961;191:1156–8.
[9] Frostell G, Larsson SJ, Lodding A, Odelius H, Petersson LG. SIMS study of element concentration profiles in enamel and dentin. Scand J Dent Res 1977;85:18–21.
[10] Norén JG, Lodding A, Odelius H, Linde A. Secondary ion mass spectrometry of human deciduous enamel. Distribution of Na, K, Mg, Sr, F and Cl. Caries Res 1983;17:496–502.
[11] Chandra S, Fullmer CS, Smith CA, Wasserman RH, Morrison GH. Ion microscopic imaging of calcium transport in the intestinal tissue of vitamin D-deficient and vitamin D-replete chickens: a 44Ca stable isotope study. Proc Natl Acad Sci 1990;87:5715–9.
[12] Chandra S, Ausserer WA, Morrison GH. Subcellular imaging of calcium exchange in cultured cells with ion microscopy. J Cell Sci 1992;102:417–25.
[13] Mantus DS, Morrison GH. Chemical imaging in biology and medicine using ion microscopy. Microchim Acta 1991;104:515–22.
[14] Todd PJ, McMahon JM, Short RT. Secondary ion emission and images from a biologic matrix. Int J Mass Spectrom Ion Proc 1995;143:131–45.
[15] Lundgren T, Persson LG, Engström EU, Chabala J, Levi-Setti R, Norén JG. A secondary ion mass spectroscopic study of the elemental composition pattern in rat incisor dental enamel during different stages of ameloblast differentiation. Arch Oral Biol 1998;43:841–8.
[16] Viriot L, Peterková R, Vonesch JL, Peterka M, Ruch JV, Lesot H. Mouse molar morphogenesis revisited by 3D reconstruction: III. Spatial distribution of mitoses and apoptoses up to bell-staged first lower molar teeth. Int J Dev Biol 1997;41:679–90.

[17] Verdelis K, Crenshaw MA, Paschalis EP, Doty S, Atti E, Boskey AL. Spectroscopic imaging of mineral maturation in bovine dentin. J Dent Res 2003;82:697–702.
[18] Verdelis K, Lukashova L, Wright JT, Mendelsohn R, Peterson MG, Doty S, et al. Maturational changes in dentin mineral properties. Bone 2007;40:1399–407.
[19] Schour I, Hoffman MM. Studies in tooth development: II. The rate of apposition of enamel and dentin in man and other mammals. J Dent Res 1935;15:161–75.
[20] Kang D, Amarasiriwardena D, Goodman AH. Application of laser ablation-inductively coupled plasma-mass spectrometry (LA-ICP-MS) to investigate trace metal spatial distributions in human tooth enamel and dentine growth layers and pulp. Anal Bioanal Chem 2004;378:1608–15.
[21] Grynpas MD, Marie PJ. Effects of low doses of strontium on bone quality and quantity in rats. Bone 1990;11:313–9.
[22] Marie PJ, Hott M, Modrowski D, de Pollak C, Guillemain J, Deloffre P, et al. An uncoupling agent containing strontium prevents bone loss by depressing bone resorption and maintaining bone formation in estrogen-deficient rats. J Bone Miner Res 1993;8:607–15.
[23] Boivin G, Deloffre P, Perrat B, Panczer G, Boudeulle M, Mauras Y, et al. Strontium distribution and interactions with bone mineral in monkey iliac bone after strontium salt (S 12911) administration. J Bone Miner Res 1996;11:1302–11.
[24] Farlay D, Boivin G, Panczer G, Lalande A, Meunier PJ. Long-term strontium ranelate administration in monkeys preserves characteristics of bone mineral crystals and degree of mineralization of bone. J Bone Miner Res 2005;20:1569–78.
[25] Meunier PJ, Slosman DO, Delmas PD, Sebert JL, Brandi ML, Albanese C, et al. Strontium ranelate: dose-dependent effects in established postmenopausal vertebral osteoporosis—a 2-year randomized placebo controlled trial. J Clin Endocrinol Metab 2002;87:2060–6.
[26] Meunier PJ, Roux C, Seeman E, Ortolani S, Badurski JE, Spector TD, et al. The effects of strontium ranelate on the risk of vertebral fracture in women with postmenopausal osteoporosis. N Engl J Med 2004;350:459–68.
[27] Reginster JY, Seeman E, de Vernejoul MC, Adami S, Compston J, Phenekos C, et al. Strontium ranelate reduces the risk of nonvertebral fractures in postmenopausal women with osteoporosis: Treatment of Peripheral Osteoporosis (TROPOS) study. J Clin Endocrinol Metab 2005;90:2816–22.